It may be worthwhile to apply the procedure described in this paper to heavy atom derivatives of complex materials such as proteins. The relative scattering power of the heavy atoms and the collection of as many data as possible are important considerations.

Dr Isabella Karle and Mrs Judith Flippen have collaborated in carrying out the experimental tests. Their fine cooperation is very much appreciated. We are grateful to Mr. Stephen Brenner for programming the calculation of the recycling procedure.

References

COULTER, C. L. (1965). *J. Mol. Biol.* **12**, 292.
GASSMANN, J. (1966). *Acta Cryst.* **21**, A6.
HOPPE, W. (1957). *Z. Elektrochem.* **61**, 1076.
HOPPE, W. (1963). *Z. Kristallogr.* **118**, 121.
HOPPE, W., HUBER, R. & GASSMANN, J. (1963). *Acta Cryst.* **16**, A4.
HOPPE, W. & WILL, G. (1960). *Z. Kristallogr.* **113**, 104.
HUBER, R. & HOPPE, W. (1965). *Chem. Ber.* **98**, 2403.
KARLE, I. L., KARLE, J. & ESTLIN, J. A. (1967). *Acta Cryst.* **23**, 494.
KARLE, J. (1966). *Acta Cryst.* **21**, 273.
KARLE, J., FLIPPEN, J. & KARLE, I. L. (1967). *Z. Kristallogr.* To be published.
KARLE, J. & HAUPTMAN, H. (1956). *Acta Cryst.* **9**, 635.
KARLE, J. & KARLE, I. L. (1966). *Acta Cryst.* **21**, 849.
NORDMAN, C. E. & NAKATSU, K. (1963). *J. Amer. Chem. Soc.* **85**, 353.
NORDMAN, C. E. (1966). *Trans. Amer. Cryst. Assn.* **2**, 29.
SIM, G. A. (1960). *Acta Cryst.* **13**, 511.
WOOLFSON, M. M. (1956). *Acta Cryst.* **9**, 804.
YONEMITSU, O., WITKOP, B. & KARLE, I. L. (1967). *J. Amer. Chem. Soc.* **89**, 1039.

Acta Cryst. (1968). B**24**, 186

Atomic Ordering in Binary *A*15-Type Phases

BY E.C. VAN REUTH*
Naval Ship Research and Development Center, Annapolis, Maryland, U.S.A.

AND R.M. WATERSTRAT
Dental Research Section, National Bureau of Standards, Washington, D.C., U.S.A.

(*Received* 29 *November* 1966 *and in revised form* 10 *June* 1967)

The degree of long-range order has been determined for 20 binary *A*15-type phases containing various transition elements. A tendency toward a lower degree of order was noted as the component elements were chosen successively from columns in the periodic table approaching the Mn column. A comparison of the ordering in the *A*15-type phases with the ordering previously reported for various binary σ phases suggests that the remarkable stability of these phases may result from an interdependence between the electronic structure and the ability of the atoms to undergo deformations in conforming to geometrical packing requirements.

The *A*15-type structure may be regarded as belonging to a group of crystal structures which have common crystallographic features and occur in many alloy phases formed by the transition elements. These structures have been described in terms of four characteristic atomic coordination polyhedra (Kasper polyhedra) possessing coordination numbers of 12, 14, 15 and 16 respectively (Kasper, 1956; Shoemaker, Shoemaker & Wilson, 1957; Frank & Kasper, 1958, 1959; Komura, Sly & Shoemaker, 1960; Shoemaker & Shoemaker, 1963). If atomic packing considerations are an important factor in stabilizing these phases, one might expect an atomic ordering to occur such that the icosahedral 12-coordinated polyhedra would contain the smaller atoms while the larger atoms enter sites with 14, 15 or 16 coordinations. Such an ordering of atoms has been observed in many of these structures [a summary is given in a recent paper by Shoemaker, Shoemaker & Mellor (1965)] but attempts to measure the extent of atomic ordering at each atomic site have often been restricted by the necessity of simultaneously determining the atomic position parameters. In the *A*15 structure type, however, the atomic position parameters are fixed by the symmetry requirements of space group *Pm*3*n* so that for the 'ideal' (A_3B) stoichiometric composition the B atoms are in positions 2(*a*) (0,0,0) and the A atoms are in positions 6(*c*) $(0,\frac{1}{4},\frac{1}{2})$. Consequently, measurements of atomic ordering in these phases can be made with greater accuracy and with less ambiguity since there are only two crystallographic lattice sites in this structure.

Geller, Matthias & Goldstein (1955) have reported a high degree of atomic ordering in Nb_3Os, Nb_3Ir, Nb_3Pt and V_3Sn, but only a partial ordering in Ta_3Sn.

* On leave of absence to Kamerlingh Onnes Laboratory, University of Leiden, Leiden, The Netherlands, for the 1966–67 academic year.

The partial ordering in Ta_3Sn has been confirmed by Courtney, Pearsall & Wulff (1965*a*) who have also reported evidence that vacant atomic sites exist in this phase after a vacuum heat treatment. Matthias, Geballe, Willens, Corenzwit & Hull (1965) have produced a considerable amount of disorder in the phase Nb_3Ge by using special rapid-quenching techniques.

In many other investigations the *A*15-type phases have apparently been assumed to be completely ordered since their composition ranges are relatively narrow and frequently confined to the 'ideal' (A_3B) composition. The recent discoveries of binary *A*15-type phases which are stable at compositions deviating significantly from the 'ideal' composition (Darby & Zegler, 1962; Hartly, Parsons & Seedly, 1964; Ray & Parsons, 1966; Sadogopan, Gatos & Giessen, 1965; Raub & Röschel, 1966) suggests, however, that the crystallographic sites need not be occupied exclusively by only one chemical element. In some cases considerable disorder exists even at or near the 'ideal' composition (Waterstrat & van Reuth, 1966).

This study of the atomic ordering in twenty binary *A*15-type phases was undertaken primarily to ascertain those factors which may be responsible for the atomic ordering and which may perhaps also be responsible for the remarkable stability of the *A*15-type phases.

Experimental procedure

Alloy preparation

All except three of our alloys were melted in an electric arc furnace using a non-consumable tungsten electrode. The three alloys in the Mo–Pt, Cr–Pt, and Cr–Os systems which are designated as specimens no. 1 in Table 2 were prepared by powder metallurgy methods. Melting losses were always less than one per cent by weight. Annealing treatments were carried out usually in a vacuum furnace equipped with tantalum heating elements at pressures of between 10^{-6} and 10^{-7} torr. At the lower temperatures (< 1200 °C) annealing was done in evacuated quartz tubes. In order to induce

Table 1. *Purity of metals used in alloy preparation*

Titanium	99·9%
Vanadium	99·95
Chromium	99·999
Niobium	99·9
Molybdenum	99·9
Ruthenium	99·9
Rhodium	99·95
Palladium	99·9
Osmium	99·999
Iridium	99·95
Platinum	99·99
Gold	99·99

Table 2. *Nominal starting compositions, annealing treatments, and long-range order parameters* (*S*)

Nominal composition	Specimen no.	Annealing temperature (°C)	Annealing time	*S*
$Cr_{79}Pt_{21}$	1	1300*	9 hours	0·90 ± 0·05
	2	1200	3 days	1·00 ± 0·02
Cr_3Ir	1	'as-cast'*		0·89 ± 0·02
	2	'as-cast'		0·89 ± 0·02
$Cr_{72}Os_{28}$	1	1400†	8 hours	0·64 ± 0·05
	2	1400	24 hours	0·66 ± 0·02
Cr_3Rh	1	1200	3 days	0·83 ± 0·04
$Cr_{72}Ru_{28}$	1	800	6 weeks	0·55 ± 0·04
V_3Au	1	'as-cast'		0·99 ± 0·02
	2	'as-cast'*		0·92 ± 0·02
V_3Pt	1	'as-cast'*		0·95 ± 0·02
	2	'as-cast'		0·98 ± 0·02
V_3Ir	1	'as-cast'		0·94 ± 0·02
V_3Pd	1	800	1 month	0·69 ± 0·04
V_3Rh	1	1200	3 days	
		1100	2 weeks	0·96 ± 0·04
Ti_3Au	1	'as-cast'		0·97 ± 0·02
Ti_3Pt	1	'as-cast' *		0·97 ± 0·02
	2	'as-cast'		0·99 ± 0·02
Ti_3Ir	1	'as-cast'		1·00 ± 0·02
	2	'as-cast'*		0·91 ± 0·02
Mo_4Pt	1	1600†	48 hours	0·98 ± 0·05
	2	1600	24 hours	0·98 ± 0·05
Mo_3Ir	1	1800	2 days	0·87 ± 0·05
Mo_3Os	1	2000	2 days	0·81 ± 0·05
Nb_3Au	1	'as-cast'		0·89 ± 0·05
Nb_3Pt	1	1600	5 days	0·93 ± 0·05
Nb_3Ir	1	2000	3 hours	0·95 ± 0·05
Nb_3Os	1	1800	2 days	0·90 ± 0·05
		1600	5 days	

Note: All arc-melted alloy specimens were given a final annealing at 800 °C for one hour followed by slow cooling except those marked * which were allowed to remain in the 'as-cast' condition following arc-melting and solidification in a water-cooled copper hearth. Alloy specimens prepared by powder metallurgy were cooled from their sintering temperatures by turning off the furnace power. These are marked † and were not given a final anneal at 800 °C.

maximum ordering it was decided to anneal all alloys for one hour at 800°C before a final slow cooling. After annealing, the alloys were crushed in a hardened steel rod mill to a 20–50 micron particle size. This particle size was chosen to minimize preferred orientation effects on the X-ray diffraction patterns and at the same time, to avoid line broadening effects due to fine particle sizes. Spectrographic analyses of each powder sample revealed no major contaminants or impurities. The nominal purities of all starting materials are given in Table 1.

X-ray diffraction

The degree of long-range order (LRO) in each sample was studied by means of data obtained on a diffractometer with nickel-filtered copper radiation. The powders were packed with a uniform pressure into a tray of 24 mm diameter and 1·3 mm depth which was rotated about an axis normal to the specimen surface during the data-taking period. Precision lattice parameters were later obtained by adding an internal standard of either silver ($a_0 = 4{\cdot}08625$ Å) or tungsten ($a_0 = 3{\cdot}16504$ Å) and using a least-squares fitting of the data with greater weight assigned to the lines occuring at high Bragg angles (Table 3). Standard Debye–Scherrer X-ray patterns were also obtained to assist in detecting extremely weak lines and possible effects due to preferred orientation. These could reduce the reliability of the data obtained by the diffractometer.

It was found that the difficulty involved in completely removing any preferred orientation in the powdered samples was a major factor limiting the accuracy of our determination of the long-range order parameters. This difficulty has also been encountered by previous investigators (Courtney, Pearsall & Wulff, 1965*b*). Fortunately, there is at least one unmistakable check that can be made for preferred orientation effects on all patterns. The long-range order parameter contributions to the intensities of the 200 and 211 reflections are identical (Table 4) and the value of this observed intensity ratio is thus a good measure of preferred orientation effects.

Table 3. *Lattice parameters for alloys studied**

Alloy	No.	a_0 (Å) ±0·0001
Ti_3Ir	1	5·0082
	2	5·0087
Ti_3Pt	1	5·0309
	2	5·0327
Ti_3Au	1	5·0974
V_3Rh	1	4·7852
V_3Pd	1	4·8254
V_3Ir	1	4·7876
V_3Pt	1	4·8166
	2	4·8166
V_3Au	1	4·8813
	2	4·8807
$Cr_{72}Ru_{28}$	1	4·6768
Cr_3Rh	1	4·6731
$Cr_{72}Os_{28}$	1	4·6799
	2	4·6842
Cr_3Ir	1	4·6808
	2	4·6810
$Cr_{79}Pt_{21}$	1	4·6997
	2	4·7058
Nb_3Os	1	5·1348
Nb_3Ir	1	5·1333
Nb_3Pt	1	5·1524
Nb_3Au	1	5·2024
Mo_3Os	1	4·9689
Mo_3Ir	1	4·9682
Mo_4Pt	1	4·9878

* All lattice parameters were measured at a temperature of 25±1°C.

Table 4. *Long-range order parameter contributions to A15-structure factors*

hkl	*S* Contribution to *F*
110	$2S(f_B-f_A)$
200	$S(f_B-f_A)\pm(3f_A+f_B)$
210	$S(f_B-f_A)-(3f_A+f_B)$
211	$S(f_B-f_A)+(3f_A+f_B)$
220	$2S(f_B-f_A)$
310	$2S(f_B-f_A)$
222	$3S(f_B-f_A)-(3f_A+f_B)$
320	$S(f_A-f_B)+(3f_A+f_B)$
321	$S(f_B-f_A)+(3f_A+f_B)$
400	$2(3f_A+f_B)$
411, 330	$2S(f_B-f_A)$
420	$S(f_B-f_A)+(3f_A+f_B)$
421	$S(f_B-f_A)-(3f_A+f_B)$
332	$S(f_B-f_A)+(3f_A+f_B)$
422	$2S(f_B-f_A)$
510, 431	$2S(f_B-f_A)$
520, 432	$S(f_A-f_B)+(3f_A+f_B)$
521	$S(f_B-f_A)+(3f_A+f_B)$
440	$2(3f_A+f_B)$
530, 433	$2S(f_B-f_A)$
600, 442	$S(f_B-f_A)+(3f_A+f_B)$
610	$S(f_B-f_A)-(3f_A+f_B)$
611, 532	$S(f_B-f_A)+(3f_A+f_B)$

In all cases, the X-ray patterns were indexed completely with all peaks accountable. In no instances were lines observed which would correspond to the 100 or 111 peaks in confirmation of the requirements of the *Pm*3*n* space group. A few of the specimens were found to produce some extremely weak extraneous peaks which did not superimpose on the basic *A*15 pattern. These were identified as resulting from small quantities of a second phase. Aside from these peaks the diffractometer traces were normal in all respects. In particular there were no indications of residual strains, abnormal line broadening, splitting of lines at high angles, or forbidden reflections and all peaks were close to the usual Gaussian shape. Peak intensities were measured with a planimeter on the original slow traces obtained with the diffractometer.

Model calculations

A computer program was devised to assimilate the data in such a manner as to select the best ordering model to fit the data. This program contained atomic scattering factors obtained from *International Tables for X-ray Crystallography* (1962). Anomalous dispersion corrections were applied for all of the elements studied using the values given by Cromer (1965). The

usual analytical expression for the Lorentz polarization factors and multiplicity factors were used in the intensity calculations. A provision was also contained in the program to accommodate off-stoichiometric model calculations. This was done by inserting a chemical composition factor in the intensity equation (see Appendix). Such a procedure is probably valid for small deviations (a few per cent) from the 'ideal' (A_3B) stoichiometric composition.

In deciding whether to include a temperature factor in the calculations ,as is usually done, it was recognized that the presence of residual preferred orientation might tend to obscure the effects of a temperature factor in data obtained only at room temperature. We therefore re-ran each pattern at liquid nitrogen temperature in order to obtain a more realistic estimate of temperature effects on the peak intensities. It was found that the relative intensities of the first four peaks occurring at low Bragg angles remain essentially unchanged at 79°K but that the intensity of peaks occurring at higher angles may be significantly increased. Angular dependent terms, however, are partially offset by our using, as raw data, the *ratios* of adjacent peak intensities rather than their individual values. One might estimate the temperature factor utilizing the data obtained at 79°K but this introduces some uncertainty due to the preferred orientation effects and we therefore did not include a temperature factor in our calculations.

The observed data were compared first with ten different calculated models having long range order parameters (S) from 0·0 (complete disorder) to 1·0 (complete order) in 0·1 increments (see Appendix). When the region of maximum interest was found, the computer then compared the observed data with 20 other calculated models at 0·01 increments of S. A reliability factor was calculated for each of these 20 model comparisons and the 'best' ordered model was selected as the one having the lowest value for its reliability index. The reliability index used in these calculations was:

$$R = \frac{1}{\Sigma W_i} \sum_{i=1}^{i=N} W_i \frac{[\varrho_{oi} - \varrho_{ci}]^2}{\varrho_{oi}\varrho_{ci}} \qquad (1)$$

where

- R is the reliability index for a given S value
- N is the number of observed intensity ratios
- ϱ_{oi} are the observed intensity ratios
- ϱ_{ci} are the calculated intensity ratios
- W_i is a weighting factor which was initially chosen as 10 for the 200/110, 210/200 and 211/210 intensity ratios; all other intensity ratios received weights of either 5 (ratios from 220/211 to 332/421) or one (ratios beyond 332/421).

It was subsequently found that the weighting factors as initially chosen placed far too much emphasis on the higher angle peaks which are not only inherently less sensitive to the atomic ordering (see Fig. 1) but their intensities are also substantially reduced through the uncompensated influence of the temperature factor. In order to obtain a more realistic emphasis on the lower angle peaks it appears that some correction for the temperature factor should be made. We have found, however, that satisfactory intensity agreement is obtained (Table 5) simply by changing the weighting factor (W_i) for the first three intensity ratios from 10 to 10^4 without altering the rest of the program.

After the best-fit model was selected, the calculated intensities were normalized on the basis of a value of 1000 for the 211 peak. These calculated normalized values could then be compared directly with the observed normalized values. The calculations did not consider the possible existence of lattice vacancies since density measurements on these alloys and others (Waterstrat & van Reuth, 1966) have indicated that the percentages of lattice vacancies are too small to warrant inclusion in the intensity calculations.

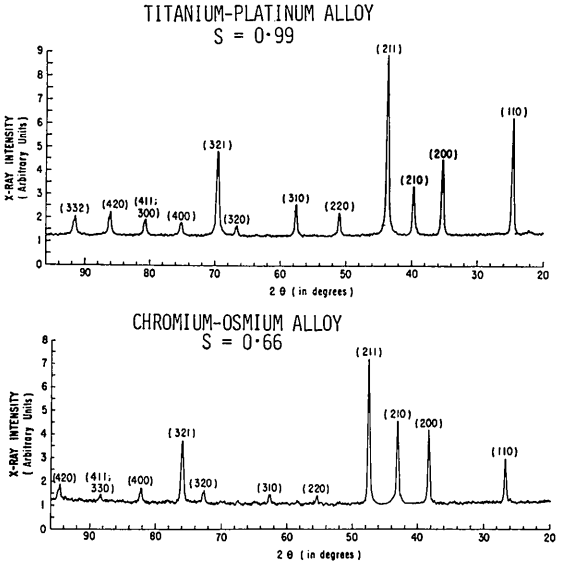

Fig. 1. X-ray pattern of a highly ordered $A15$-type phase (Ti_3Pt) compared with the pattern of a partially disordered $A15$-type phase ($Cr_{72}Os_{28}$).

Experimental results

The results of this study on the degree of long-range order in twenty samples exhibiting the $A15$ structure are shown in Table 5. Below each alloy designation there are three columns of intensity values. The first column lists the observed relative intensity values obtained from the planimetered diffractometer traces. The values shown in column two are those calculated for the selected model whose S value appears at the head of that column. The third column lists the intensity values one would expect for a completely ordered structure ($S = 1·0$). (In those instances where the computer selected an LRO parameter of 1·0, column three would be redundant and has therefore been omitted.)

Table 5. *Comparison of observed and calculated intensities for samples annealed at* 800 °C

	Cr_3Rh			$Cr_{72}Ru_{28}$			$Cr_{79}Pt_{21}$		Cr_3Ir			$Cr_{72}Os_{28}$		
hkl	I_{obs}	I_{calc} $S=$ 0·83	I_{calc} $S=$ 1·00	I_{obs}	I_{calc} $S=$ 0·55	I_{calc} $S=$ 1·00	I_{obs}	I_{calc} $S=$ 1·00	I_{obs}	I_{calc} $S=$ 0·89	I_{calc} $S=$ 1·00	I_{obs}	I_{calc} $S=$ 0·66	I_{calc} $S=$ 1·00
110	165	165	226	61	66	188	565	575	538	510	606	281	309	519
200	467	469	468	435	471	470	476	458	453	458	457	464	459	458
210	743	712	624	935	908	657	315	307	368	349	291	471	511	341
211	1000	1000	1000	1000	1000	1000	1000	1000	1000	1000	1000	1000	1000	1000
220	27	24	33	—	10	29	109	89	102	78	93	45	48	81
310	35	34	46	20	14	39	121	126	113	112	133	71	68	115
222	—	19	11	44	40	15	—	<1	—	<1	1	—	4	<1
320	138	136	118	130	173	124	69	58	64	67	55	98	100	64
321	488	475	477	466	456	458	484	503	475	503	505	509	499	503
400	144	142	134	122	152	132	133	108	116	113	107	135	130	112
411, 330	18	23	31	—	8	22	113	83	72	75	87	45	45	76
420	125	151	152	132	138	138	161	160	178	161	162	155	159	160
421	117	141	122	140	177	128	55	59	55	69	57	97	105	66
332	113	142	143	132	128	128	117	151	123	152	153	157	149	151
422	—	13	18	—	4	12	51	47	47	42	50	—	24	43
510, 431	36	42	57	14	12	36	120	145	136	130	154	90	78	133
520, 432	234	231	198	248	287	207	65	94	81	113	92	174	171	107
521	351	346	349	278	301	301	290	356	340	364	366	342	357	360
440	246	292	277	242	293	254	210	213	144	231	218	245	264	224
530, 433	—	54	74	—	14	42	125	172	85	162	190	93	96	192
600, 442		654	659		515	515		548	382	635	635	612	622	609
610														
611, 532														
R=		0·0248	0·0694		0·0086	0·5092		0·0063		0·0045	0·0439		0·0206	0·2036

	V_3Pd			V_3Rh			V_3Au			V_3Pt			V_3Ir		
hkl	I_{obs}	I_{calc} $S=$ 0·69	I_{calc} $S=$ 1·00	I_{obs}	I_{calc} $S=$ 0·96	I_{calc} $S=$ 1·00	I_{obs}	I_{calc} $S=$ 0·99	I_{calc} $S=$ 1·00	I_{obs}	I_{calc} $S=$ 0·98	I_{calc} $S=$ 1·00	I_{obs}	I_{calc} $S=$ 0·94	I_{calc} $S=$ 1·00
110	154	153	286	262	253	270	640	616	625	679	654	673	658	600	656
200	466	465	465	456	465	464	463	453	453	467	454	454	464	454	454
210	715	707	528	635	587	567	284	278	273	266	262	253	306	291	261
211	1000	1000	1000	1000	1000	1000	1000	1000	1000	1000	1000	1000	1000	1000	1000
220	28	23	44	48	36	39	113	97	98	108	101	104	119	93	101
310	38	32	60	55	51	55	149	139	140	144	143	147	166	131	144
222	18	20	6	—	9	8	—	2	2	9	2	3	—	1	3
320	137	139	103	117	114	110	44	54	53	47	51	49	60	57	51
321	503	467	468	442	481	481	488	506	506	543	507	508	548	508	509
400	152	139	123	138	132	130	98	105	104	150	104	103	106	108	104
411, 330	23	18	33	28	33	35	78	87	89	97	90	93	118	84	92
420	123	137	137	159	149	148	128	154	154	178	157	157	164	158	159
421	110	137	102	111	115	110	48	51	50	54	51	49	51	57	51
332	120	124	124	131	156	137	114	141	141	151	145	145	153	147	147
422	—	9	16	—	18	19	54	46	47	54	49	50	58	46	50
510, 431	50	26	48	69	58	58	122	138	140	180	147	151	161	138	151
520, 432	159	195	147	159	174	164	64	70	69	72	74	71	92	85	75
521	212	255	255	221	309	301	280	287	287	278	309	310	336	320	320
440	179	211	187	172	232	221	151	155	155	144	170	167	200	184	178
530, 433	20	24	44	41	30	62	121	126	128	122	144	148	117	140	152
600, 442	254	262	261	276	371	344	280	274	274	300	328	329	330	360	361
610		136	102	149	156	133		42	41	43	53	51	49	69	61
611, 532		1024	1021		2509			943	924	1312	1335	1341	1490	1808	1812
R=		0·0007	0·1952		0·0199	0·0221		0·0004	0·0007		0·0007	0·0015		0·0040	0·0148

Table 5 (*cont.*)

	Ti_3Au			Ti_3Pt			Ti_3Ir		Mo_xPt_y			Mo_3Ir		
hkl	I_{obs}	I_{calc} $S=$ 0·97	I_{calc} $S=$ 1·00	I_{obs}	I_{calc} $S=$ 0·99	I_{calc} $S=$ 1·00	I_{obs}	I_{calc} $S=$ 1·00	I_{obs}	I_{calc} $S=$ 0·98	I_{calc} $S=$ 0·98	I_{obs}	I_{calc} $S=$ 0·87	I_{calc} $S=$ 1·00
									$Mo_{80}Pt_{20}$		$Mo_{85}Pt_{15}$			
110	709	684	715	698	694	704	652	688	144	138	86	158	146	185
200	440	448	448	458	449	449	444	449	452	450	450	442	449	449
210	250	236	222	238	234	230	224	238	810	714	820	742	704	641
211	1000	1000	1000	1000	1000	1000	1000	1000	1000	1000	1000	1000	1000	1000
220	128	110	115	120	110	111	108	109	18	23	15	21	24	30
310	188	156	163	165	157	159	172	155	35	33	21	30	34	43
222	—	4	5	—	5	4	—	4	17	23	35	16	22	16
320	56	47	44	56	47	46	52	47	174	154	176	177	152	138
321	516	514	515	522	512	512	509	513	500	516	515	545	517	517
400	105	101	99	91	101	100	103	101	170	155	164	140	155	149
411, 330	114	96	99	87	96	98	116	96	13	20	13	21	21	27
420	143	151	151	134	152	152	130	153	139	155	155	140	156	156
421	41	44	41	40	44	43	23	44	130	154	177	130	153	139
332	136	135	136	123	137	137	121	138	110	141	141	126	142	142
422	50	47	49	50	48	49	58	48	—	12	7	—	11	13
510, 431	155	135	141	134	140	141	121	140	18	30	19	22	30	39
520, 432	39	53	50	59	55	54	42	57	217	207	237	153	207	189
521	230	240	240	228	252	251	229	256	248	267	267	251	271	273
440	103	120	118	120	127	126	112	131	152	212	225	140	215	208
530, 433	95	102	106	120	110	110	121	102	—	31	16	—	24	32
600, 442	172	186	186	191	205	205	198	212	165	226	226	153	233	235
610	23	24	22	30	26	26	30	28	104	105	121	93	108	99
611, 532	486	518	517	392	591	589	406	621	615	671	671	567	699	708
$R=$		0·0046	0·0117		0·0008	0·0014		0·0033		0·0107	0·0887		0·0117	0·0360

	Mo_3Os			Nb_3Au			Nb_3Pt			Nb_3Ir			Nb_3Os		
hkl	I_{obs}	I_{calc} $S=$ 0·81	I_{calc} $S=$ 1·00	I_{obs}	I_{calc} $S=$ 0·89	I_{calc} $S=$ 1·00	I_{obs}	I_{calc} $S=$ 0·93	I_{calc} $S=$ 1·00	I_{obs}	I_{calc} $S=$ 0·95	I_{calc} $S=$ 1·00	I_{obs}	I_{calc} $S=$ 0·90	I_{calc} $S=$ 1·00
110	125	120	173	193	185	225	189	188	213	189	184	200	175	157	188
200	497	450	449	452	444	444	429	445	445	468	446	445	442	446	445
210	734	752	659	630	633	578	610	630	595	620	638	614	730	680	631
211	1000	1000	1000	1000	1000	1000	1000	1000	1000	1000	1000	1000	1000	1000	1000
220	21	20	28	27	31	37	44	31	35	41	30	33	40	26	31
310	30	28	40	41	44	53	54	44	50	52	43	47	57	37	45
222	20	27	17	—	16	11	33	15	12	23	16	14	21	20	15
320	166	162	141	140	139	127	163	138	130	152	139	134	142	148	138
321	507	516	517	502	523	523	538	521	522	512	522	522	500	521	522
400	169	159	150	149	150	144	140	149	145	132	150	147	149	153	149
411, 330	22	18	25	18	27	32	25	27	30	32	27	29	43	23	27
420	160	155	156	138	152	153	171	153	153	139	153	154	135	153	153
421	156	164	143	125	134	122	150	134	126	127	136	130	127	145	134
332	127	141	142	102	136	136	102	137	137	132	137	138	104	137	137
422	—	9	12	—	12	15	13	13	14	12	13	14	7	11	13
510, 431	20	25	36	16	36	43	38	36	41	52	36	39	28	31	36
520, 432	190	222	194	109	160	145	163	163	154	155	172	161	130	180	165
521	211	271	271	188	229	235	214	235	236	220	239	240	213	239	238
440	177	222	210	133	167	160	142	172	169	141	172	174	135	182	175
530, 433	10	20	28	—	24	30	38	26	30	30	26	28	10	22	26
600, 442	170	234	234	130	167	167	135	176	177	164	186	181	151	181	180
610	97	117	102	50	65	60	58	72	66	73	73	70	66	79	72
611, 532	557	704	705	358	447	448	388	479	481	416	496	498	382	501	492
$R=$		0·0066	0·0655		0·0138	0·0338		0·0018	0·0082		0·0009	0·0045		0·0090	0·0245

The results of this work show that most of the titanium and vanadium alloys are nearly completely ordered, but that the chromium alloys exhibit a rather wide variance in the degree of LRO. Molybdenum alloys also exhibit variations in the degree of LRO but the order parameters of the niobium alloys remain relatively constant. These relationships are summarized in Fig. 2.

The order parameters obtained for the Mo–Pt *A*15 phase were between 0·96 and 1·00 depending on the weighting of the lines and on the assumed composition of this phase. The composition $Mo_{85}Pt_{15}$ has been suggested for this phase (Sadogopan, Gatos & Giessen, 1965) but an arc-melted alloy prepared by us at this composition and annealed at 1600 °C for three days contained two phases. A second sample having the nominal composition Mo_4Pt contained less of the second phase. Both samples, however, consisted mainly of the *A*15-type phase. Similarly, the alloy Cr_3Ru contained a second phase whereas a second sample, $Cr_{72}Ru_{28}$ contained less of this phase.

Specimens subjected to fast cooling (as-cast) generally had lower order parameters than those which had been slowly cooled and they exhibited differing superconducing transition temperatures (Blaugher, Hein, Cox, van Reuth & Waterstrat, 1967). This suggests a possible relationship between the LRO parameter (S) and the superconducting transition temperature (Tc) in the *A*15-type phases.

The major factor limiting the accuracy of our order parameters is the residual effects of preferred orientation which was difficult to evaluate quantitatively. By making successive runs on various samples, however, and then noting the variations in line intensities, it was possible to estimate the accuracies to some extent and these estimates are given in Table 2.

In each case where the room temperature data suggested a temperature factor contribution to the intensities, an enhancement of these intensities was observed at liquid nitrogen temperatures which was sufficient to support such a conclusion. It may be noteworthy that the temperature factor correction appears to be unusually small in the *A*15-type phases containing Ti or V as the A element and also when the A-atom positions have mixed occupancy.

Discussion

The frequent occurrence of the *A*15-type phases in alloys of the transition elements attests to the rather high degree of stability of this structure. Much of this stability seems to be associated with the mutually orthogonal chains of A atoms extending in the ⟨100⟩ directions throughout the crystal. The interatomic distances between the atoms in these chains are appreciably shorter than the C.N.12 interatomic distances derived for the pure elements and one may infer that *d*-electrons are intimately involved in the bonding. The atomic configuration of these chains is shown in Fig. 4.

Nevitt (1962) has demonstrated that a roughly linear relationship is obtained by plotting the observed 'lattice contractions' in the direction of the atom chains (D_A–d_A) against the Goldschmidt radius ratios (R_A/R_B) for the atoms in the phase. Fig. 3 is a plot similar to Nevitt's except that we have utilized the lattice parameter data obtained in the present investigation. It now appears that the lattice 'contractions' in the *A*15-type phases having a common A element (Ti, V, Cr,

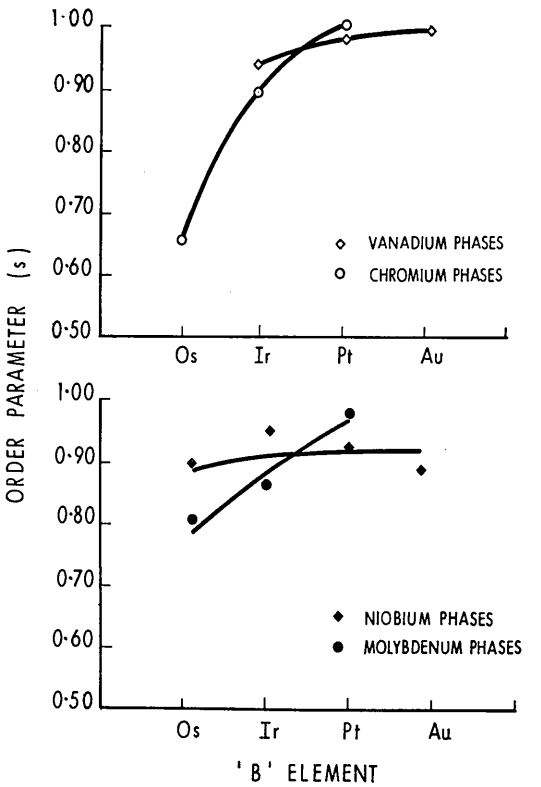

Fig. 2. Degree of atomic ordering in *A*15-type phases as a function of the position of the constituent elements in the periodic table.

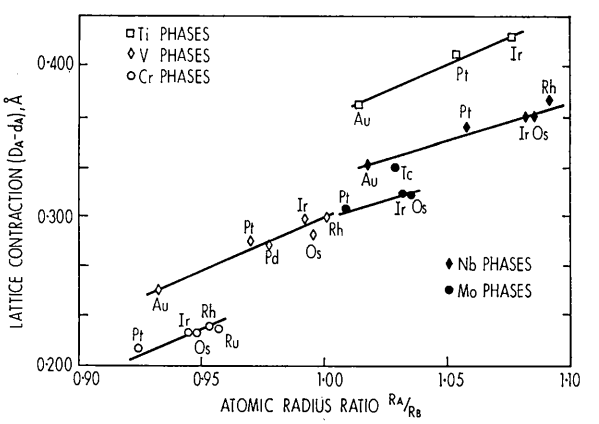

Fig. 3. A–A lattice contractions in *A*15-type phases as a function of the Goldschmidt radius ratio (R_A/R_B).

Nb, Mo) fall along separate straight lines having similar slopes. This indicates that it is not simply the Goldschmidt radius ratios which influence the observed 'contractions' in the direction of the A–A interatomic distances but also the identity of the A element itself.

If one attempts to assign characteristic 'atomic radii' to the A atoms constituting these chains one faces the problem of this apparent lack of rigidity as well as a behavior of the interatomic distances which is quite inconsistent with a concept of spherical atoms (Nevitt, 1962, 1966). This problem has been dealt with in connection with the *A*15-type structure and other complex structures by assigning both 'major' and 'minor' radii to a given atom (Shoemaker & Shoemaker, 1964) depending on the ligand coordination number. Nevitt (1966) suggests, however, that 'radius' is not a meaningful term for describing atomic size under these circumstances.

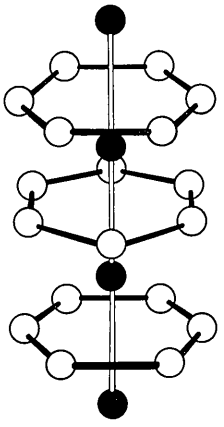

Fig. 4. Atomic configuration occurring in both the σ phases and the A15-type phases. Relative length of distances along the vertical A–A atom chain is exaggerated for the sake of clarity.

Nevertheless, if one considers the spheres to be somewhat deformable, then geometric sphere-packing concepts may be quite useful. The validity of the sphere packing principles developed by Frank & Kasper (1958, 1959) actually depend on the assumption that the atoms possess a considerable capacity for undergoing deformation. If this is the case in the actual crystal then it seems highly probable that the stability of these phases and also their atomic ordering tendencies would depend not merely on the sizes of the atoms as expressed by the atomic radius ratios (with their implicit assumption of rigid spherical atoms) but rather on the ability of the atoms to undergo sizable deformations.

Studies of atomic ordering in these phases may therefore reveal significant information regarding the ability of each elementary component to undergo the amount of atomic deformation needed in order to interchange its position with an atom from another crystallographic lattice site. The *A*15-type structure is particularly attractive for such studies since only two crystallographic sites are involved and therefore an atom which leaves one of these sites may be assumed to enter the other site. The evidence obtained in the present investigation indicates that the ability of an atom to enter any given lattice site depends to some

Table 6. *Order parameters for binary σ phases and fractional occupancy of each atomic site*

	Order parameters*						Fractional occupancy (%)				
System	2(*a*) C.N.12	4(*f*) C.N.15	8(*i*) C.N.14	8(*i*) C.N.12	8(*j*) C.N.14	Composition (atomic%B)*	2(*a*) C.N.12	4(*f*) C.N.15	8(*i*) C.N.14	8(*i*) C.N.12	8(*j*) C.N.14
V–Ni	*0·78*	0·92	0·80	*0·80*	0·96	31 Ni	85·0 Ni	2·5 Ni	6·3 Ni	86·3 Ni	1·2 Ni
	0·84	1·00	0·48	*0·89*	0·97	36 Ni	90·0 Ni	0·0 Ni	18·7 Ni	91·3 Ni	1·2 Ni
	0·75	1·00	0·23	*0·80*	0·84	39 Ni	85·0 Ni	0·0 Ni	30·0 Ni	87·5 Ni	6·2 Ni
V–Fe	*0·75*	1·00	0·53	*0·75*	0·38	40 Fe	85·0 Fe	0·0 Fe	18·7 Fe	85·0 Fe	25·0 Fe
V–Mn	*1·00*	0·32	*0·21*	*1·00*	0·18	81 Mn	100·0 Mn	55·0 Mn	85·0 Mn	100·0 Mn	66·2 Mn
Cr–Co	*0·43*	0·87	0·62	*0·39*	*0·31*	39 Co	65·0 Co	5·0 Co	15·0 Co	62·5 Co	50·0 Co
Cr–Fe	*0·35*	0·17	*0·02*	*0·24*	0·07	54 Fe	70·0 Fe	45·0 Fe	55·0 Fe	65·0 Fe	50·0 Fe
Cr–Mn	*1·00*	0·00	0·17	*1·00*	0·25	75 Mn	100·0 Mn	75·0 Mn	62·5 Mn	100·0 Mn	56·3 Mn
	0·50	0·19	*0·25*	*0·75*	0·19	80 Mn	90·0 Mn	65·0 Mn	85·0 Mn	95·0 Mn	65·0 Mn
Cr–Re	0·58	*0·38*	*0·22*	0·17	*0·06*	60 Re	25·0 Re	75·0 Re	68·8 Re	50·0 Re	62·5 Re
Nb–Ir	*1·00*	1·00	0·69	*1·00*	0·69	40 Ir	100·0 Ir	0·0 Ir	12·5 Ir	100·0 Ir	12·5 Ir
Nb–Os	*1·00*	1·00	1·00	*1·00*	0·38	40 Os	100·0 Os	0·0 Os	0·0 Os	100·0 Os	25·0 Os
Nb–Re	*1·00*	1·00	0·26	*1·00*	0·26	55 Re	100·0 Re	0·0 Re	40·6 Re	100·0 Re	40·6 Re
Mo–Ir	*0·31*	1·00	1·00	*0·74*	0·55	28 Ir	50·0 Ir	0·0 Ir	0·0 Ir	81·3 Ir	12·5 Ir
Mo–Re	*1·00*	0·55	0·09	*0·58*	0·32	55 Re	100·0 Re	25·0 Re	50·0 Re	81·2 Re	37·5 Re
	1·00	0·25	0·25	*1·00*	0·25	67 Re	100·0 Re	50·0 Re	50·0 Re	100·0 Re	50·0 Re
Mo–Os	*0·62*	1·00	0·82	*0·91*	0·64	35 Os	75·0 Os	0·0 Os	6·2 Os	93·8 Os	12·5 Os
Mo–Co	*1·00*	1·00	0·69	*1·00*	0·69	40 Co	100·0 Co	0·0 Co	12·5 Co	100·0 Co	12·5 Co
Mo–Fe	*1·00*	0·50	0·50	*1·00*	0·50	50 Fe	100·0 Fe	25·0 Fe	25·0 Fe	100·0 Fe	25·0 Fe
Mo–Mn	*1·00*	1·00	0·00	*1·00*	0·21	63 Mn	100·0 Mn	0·0 Mn	62·5 Mn	100·0 Mn	50·0 Mn

* Elements in the Mn column or to the right of the Mn column in the Periodic Table are designated as 'B elements'. Elements to the left of the Mn column are designated as 'A elements'. Order parameters are printed in italics for atom sites preferred by B elements. References: Kasper & Waterstrat (1956), Wilson & Spooner (1963), Forsyth & d'Alte da Veiga (1963), Wilson (1963), Spooner & Wilson (1964), Algie & Hall (1966).

extent on the relative positions of the interchanging elements in the periodic table. It appears that as one selects elements progressively closer to the manganese column in the periodic table, one encounters an increasing tendency toward disordering. A parallel behavior is observed in binary σ phases (Table 6) and in various other structures involving the transition elements (Shoemaker, Shoemaker & Mellor, 1965). The phase V_3Pd and perhaps a few others seem to be peculiar exceptions to this rule and will require further study.

In view of the considerable capacity for disordering exhibited by several of the *A*15-type phases (Table 7) it is somewhat surprising that the majority of these phases occur at the 'ideal' (A_3B) stoichiometric composition. This behavior has led to descriptions of the *A*15-type phases as belonging to a group of structures characterized by simple and more or less invariant stoichiometric ratios (Greenfield & Beck, 1954; Nevitt, 1962, 1966). Such descriptions, however, appear to be oversimplified since non-stoichiometric *A*15-type phases have now been reported in the binary systems Mo–Tc (Darby & Ziegler, 1962), Ta–Pt (Hartly, Parsons & Seedley, 1964; Ray & Parsons, 1966), Mo–Pt (Sadogopan, Gatos & Giessen, 1965), V–Os (Raub & Röschel, 1966), Cr–Pt and Cr–Os (Waterstrat & van Reuth, 1966). A careful reinvestigation of some of the previously reported *A*15-type phases may reveal other examples of departure from the 'ideal' stoichiometry.

It appears that in certain cases the *A*15-type phases may even have compositions which shift in a regular manner from system to system (Waterstrat & van Reuth, 1966); a behavior similar to that observed in various σ phases and considered by many investigators as evidence that σ phases can be regarded as 'electron compounds' (Sully, 1951–1952; Rideout, Manly, Kamen, Lement & Beck, 1951; Greenfield & Beck, 1954).

The present results, however, suggest that atomic packing considerations are of major importance in stabilizing these phases. Nevertheless, the formation of appropriate atom sizes might be facilitated within certain ranges of 'electron concentration'. The remarkable stability of the σ and *A*15-type structures would therefore result not primarily from the interaction of free electrons with the Brillouin zones as in the classical 'electron compound' picture, but rather from the interdependence between electronic structure and the ability of the atoms to conform to geometrical packing requirements.

APPENDIX

If the Bragg–Williams order parameter is to be used for 'non-ideal' compositions one must assign different values of this parameter to each crystallographic position. In crystal structures containing more than two crystallographic positions, or more than two components, the order parameters on the different atom sites will, in general, be unequal and, consequently, the order parameter must be defined for each position. One must use only *positive* values however since one is defining the *preference* of an atom for a given position and not the tendency of the atom to *avoid* the position.

The Bragg–Williams order parameter may be written:

$$S_A = \frac{r_\alpha - F_A}{1 - F_A} \tag{2}$$

$$S_B = \frac{r_\beta - F_B}{1 - F_B}, \tag{3}$$

Table 7. *Order parameters for binary A15-type phases (annealed at* 800 °C) *and fractional occupancy of each atomic site*

System	Order parameter* Atomic site 6(*c*) C.N.14	2(*a*) C.N.12	Composition (atomic %B)*	Fractional occupancy (%) Atomic site 6(*c*) C.N.14	2(*a*) C.N.12
Ti–Au	0·97	*0·97*	25 Au	0·7 Au	97·8 Au
Ti–Pt	0·99	*0·99*	25 Pt	0·2 Pt	99·3 Pt
Ti–Ir	1·00	*1·00*	25 Ir	0·0 Ir	100·0 Ir
V–Au	0·99	*0·99*	25 Au	0·2 Au	99·3 Au
V–Pt	0·98	*0·98*	25 Pt	0·5 Pt	98·5 Pt
V–Ir	0·94	*0·94*	25 Ir	1·5 Ir	95·5 Ir
Cr–Pt	1·00	*0·80*	21 Pt	0·0 Pt	84·0 Pt
Cr–Ir	0·89	*0·89*	25 Ir	2·7 Ir	91·8 Ir
Cr–Os	0·57	*0·66*	28 Os	12·2 Os	75·6 Os
V–Pd	0·69	*0·69*	25 Pd	7·7 Pd	76·8 Pd
V–Rh	0·96	*0·96*	25 Rh	1·0 Rh	97·0 Rh
Cr–Rh	0·83	*0·83*	25 Rh	4·2 Rh	87·3 Rh
Cr–Ru	0·47	*0·55*	28 Ru	14·8 Ru	67·6 Ru
Nb–Au	0·89	*0·89*	25 Au	2·7 Au	91·8 Au
Nb–Pt	0·93	*0·93*	25 Pt	1·7 Pt	94·8 Pt
Nb–Ir	0·95	*0·95*	25 Ir	1·2 Ir	96·3 Ir
Nb–Os	0·90	*0·90*	25 Os	2·5 Os	92·5 Os
Mo–Pt	0·98	*0·74*	20 Pt	0·4 Pt	78·8 Pt
Mo–Ir	0·87	*0·87*	25 Ir	3·2 Ir	90·3 Ir
Mo–Os	0·81	*0·81*	25 Os	4·7 Os	85·8 Os

* See footnote to Table 6.

where S_A and S_B are the Bragg–Williams order parameters for the A sites and the B sites respectively.

r_α is the fraction of A sites occupied by a-atoms
r_β is the fraction of B sites occupied by b-atoms
F_A is the fraction of a-atoms in the phase
F_B is the fraction of b-atoms in the phase.

In our computer program we adopted certain simplifying assumptions in dealing with 'non-stoichiometric' compositions. In order to avoid solving for a separate order parameter on each atom site, we have redefined the order parameter in a manner which differs somewhat from the usual definition as given in the Bragg–Williams equation. Our redefined order parameter retains an assigned value of zero as corresponding to a completely disordered alloy, but instead of defining $S=1$ as the value for a *completely ordered* alloy we have defined this value as corresponding to the *maximum* amount of ordering possible considering the alloy composition.

In a binary non-stoichiometric alloy this simply means that the atom position which can *never* be completely filled by one type of atom is assigned an order parameter value of one when the position is filled to the *maximum* extent permitted by the alloy composition. The other position, of course, must be *completely filled* at this point with one atom type and its order parameter would therefore correspond to the usual Bragg–Williams definition, or in other words, to a value of *one* also. Thus, by redefining the order parameter in this manner, a single order parameter suffices to describe the extent of atomic ordering on both atom sites as it varies from random occupancy to complete ordering. The computer may then obtain a single solution in terms of this redefined order parameter. The *single* value so obtained may subsequently be converted to *separate* values describing the extent of ordering on each atom site in terms of the usual Bragg–Williams definition given by equations (2) and (3). This may be done by equating the Bragg–Williams order parameter (S_A or S_B) to a constant (K_A or K_B) times the single value obtained for the redefined order parameter (S'). Thus

$$S_A = K_A S' \tag{4}$$

$$S_B = K_B S' . \tag{5}$$

For a non-stoichiometric composition, either K_A or K_B must equal one but K_A cannot be equal to K_B. One may solve for K_A or K_B using the values of S_A or S_B and the value of S' corresponding to maximum ordering. The value of S_A or S_B corresponding to maximum ordering in the site not completely filled can be obtained using equations (2) and (3) by using values of r_α or r_β which correspond to the maximum filling of this site.

In making these simplifications we have assigned a modifying constant to the atomic form factor for the position which cannot be completely filled by one type of atom. This constant changes the form factor so that when the redefined order parameter for this position equals one the scattering corresponds to what one would expect for the amount of dilution obtained by the partial filling. This simplification ignores the slight differences in angular dependence of the form factor which would exist if a weighted average of each form factor were used. In the case of small deviations from the ideal stoichiometry, however, (only a few per cent) this error is probably not significant and is certainly small relative to the overall experimental error. For larger deviations from the 'ideal' stoichiometry, the weighted average of the two form factors must, of course, be used.

It is a pleasure to acknowledge the diligent efforts of Mr J. H. Brady and Miss R. Usatchew of the Naval Ship Research and Development Center in the X-ray diffractometry. The precision lattice parameters in Table 4 were obtained by Mr H. E. Swanson at the National Bureau of Standards.

The high purity vanadium used in this study was kindly furnished by the U.S. Bureau of Mines.

References

ALGIE, S. H. & HALL, E. O. (1966). *Acta Cryst.* **20**, 142.
BLAUGHER, R. D., HEIN, R. A., COX, J., VAN REUTH, E. C. & WATERSTRAT, R. M. (1967). To be published.
COURTNEY, T. H., PEARSALL, G. W. & WULFF, J. (1965*a*). *Trans. AIME*, **233**, 212.
COURTNEY, T. H., PEARSALL, G. W. & WULFF, J. (1965*b*). *J. Appl. Phys.* **36**, 3256.
CROMER, D. T. (1965). *Acta Cryst.* **18**, 17.
DARBY, J. B. & ZEGLER, S. T. (1962). *J. Phys. Chem. Solids*, **23**, 1825.
FORSYTH, J. B. & D'ALTE DA VEIGA, L. M. (1963). *Acta Cryst.* **16**, 509.
FRANK, F. C. & KASPER, J. S. (1958). *Acta Cryst.* **11**, 184.
FRANK, F. C. & KASPER, J. S. (1959). *Acta Cryst.* **12**, 483.
GELLER, S., MATTHIAS, B. T. & GOLDSTEIN, R. (1955). *J. Amer. Chem. Soc.* **77**, 1502.
GREENFIELD, P. & BECK, P. A. (1954). *Trans. AIME*, **200**, 253.
HARTLY, C. S., PARSONS, L. D. & SEEDLY, J. E., JR. (1964). *J. Met.* **16**, 119.
International Tables for X-ray Crystallography (1962). Vol. III, Table 3.3.1A. Birmingham: Kynoch Press.
KASPER, J. S. (1956). A.S.M. Seminar on Theory of Alloy Phases. *Trans. ASM*, **48**A, 264.
KASPER, J. S. & WATERSTRAT, R. M. (1956). *Acta Cryst.* **9**, 289.
KOMURA, Y., SLY, W. G. & SHOEMAKER, D. P. (1960). *Acta Cryst.* **13**, 575.
MATTHIAS, B. T., GEBALLE, T. H., WILLENS, R. H., CORENZWIT, E. & HULL, G. W., JR. (1965). *Phys. Rev.* **139**, A1501.
NEVITT, M. V. (1962). *AIME Symposium on Electronic Structure and Alloy Chemistry of the Transition Elements*, p. 123. New York: Interscience Publishers.
NEVITT, M. V. (1966). *Intermetallic Compounds*, p. 220. New York: John Wiley.

RAUB, E. & RÖSCHEL, E. (1966). *Z. Metallk.* **57**, 470.
RAY, A. E. & PARSONS, L. D. (1966). Private communication.
RIDEOUT, S., MANLY, W. D., KAMEN, E. L., LEMENT, B. S. & BECK, P. A. (1951). *Trans. AIME*, **191**, 872.
SADOGOPAN, V., GATOS, H. C. & GIESSEN, B. C. (1965). *J. Phys. Chem. Solids*, **26**, 1687.
SHOEMAKER, C. B. & SHOEMAKER, D. P. (1963). *Acta Cryst.* **16**, 997.
SHOEMAKER, C. B. & SHOEMAKER, D. P. (1964). *Trans. AIME*, **230**, 486.
SHOEMAKER, C. B., SHOEMAKER, D. P. & MELLOR, J. (1965). *Acta Cryst.* **18**, 37.
SHOEMAKER, D. P., SHOEMAKER, C. B. & WILSON, F. C. (1957). *Acta Cryst.* **10**, 1.
SPOONER, F. J. & WILSON, C. G. (1964). *Acta Cryst.* **17**, 1533.
SULLY, A. H. (1951–1952). *J. Inst. Metals*, **80**, 173.
WATERSTRAT, R. M. & VAN REUTH, E. C. (1966). *Trans. AIME*, **236**, 1232.
WILSON, C. G. (1963). *Acta Cryst.* **16**, 724.
WILSON, C. G. & SPOONER, F. J. (1963). *Acta Cryst.* **16**, 230.

Acta Cryst. (1968). B**24**, 196

Structure du Radical Nitroxyde Tetraméthyl-2,2,6,6-piperidinol-4-oxyle-1

PAR J. LAJZÉROWICZ-BONNETEAU
Laboratoire de spectrométrie physique, laboratoire associé au C.N.R.S., Faculté des Sciences, 38 *Grenoble, France*

(*Reçu le* 13 *juin* 1967)

Crystals of 2,2,6,6-tetramethylpiperidin-4-ol-1-oxide, a stable piperidine free radical, are monoclinic. The space group is *Cm* with two molecules in a cell. The structure has been determined by the (010) Patterson section and Patterson projections. The molecule, in special position, has a chair conformation. The group $\begin{matrix} C \\ \diagdown \\ NO^{\cdot} \\ \diagup \\ C \end{matrix}$ is not planar. The molecules are associated by hydrogen bonds and form chains parallel to **a**.

Introduction

Le tétramethyl-2,2,6,6-pipéridinol-4-oxyle-1, ou 'tanol' (Fig. 1), est un des nombreux radicaux libres stables du type nitroxyde, hétérocycliques saturés, synthétisés et étudiés au Laboratoire de chimie organique physique (Centre d'Études Nucléaires de Grenoble).

Ces composés font actuellement l'objet de nombreuses études: propriétés chimiques, résonance paramagnétique électronique, résonance magnétique nucléaire, spectres optiques, mesures magnétiques, chaleurs spécifiques. Du point de vue cristallographique, deux études seulement sont à signaler concernant ce type de radicaux:

La structure du di-*p*-anisyl nitroxyde par Hanson (1953) (pour ce composé $R_2NO^{\cdot}$, les groupements R étant aromatiques, les problèmes posés sont différents).

La structure en phase gazeuse par diffraction des électrons du di-t-butyl nitroxyde (Andersen & Andersen, 1966).

Nous désirons connaître les conformations du cycle pipéridinique et du groupement $>NO^{\cdot}$, le mode d'empilement des molécules et le rôle des liaisons hydrogène, la répartition des radicaux nitroxydes dans le cristal.

Methodes expérimentales

Préparation – morphologie

Nous renvoyons, pour la préparation, à l'article de Brière, Lemaire & Rassat (1965). Les cristaux se présentent sous forme d'aiguilles jaunes de 1/10 de mm² de section, de quelques millimètres de longueur; la direction d'allongement des aiguilles est l'axe *a*. Des monocristaux plus gros sont obtenus à partir d'une solution saturée d'éther de pétrole maintenue à température constante; nous pouvons découper des aiguilles selon les trois axes cristallographiques.

Rayons X

Les paramètres sont déterminés avec des clichés de poudre faits sur une chambre à focalisation associée à un monochromateur. La longueur d'onde est Co $K\alpha_1$; l'étalon utilisé est le germanium.

Les taches de diffraction d'un monocristal sont recueillies sur des clichés de Weissenberg (équi-inclinaison). Les intensités sont mesurées visuellement: échelles d'intensité, technique à plusieurs films. Aucune correction d'absorption n'est faite.

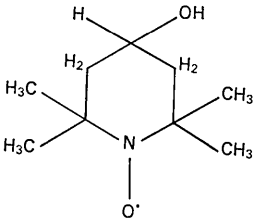

Fig. 1. Tétramethyl-2,2,6,6-pipéridinol-4-oxyle-1.